

This is the accepted manuscript made available via CHORUS. The article has been published as:

Strictly one-dimensional electron system in Au chains on Ge(001) revealed by photoelectron k-space mapping

S. Meyer, J. Schäfer, C. Blumenstein, P. Höpfner, A. Bostwick, J. L. McChesney, E. Rotenberg, and R. Claessen

Phys. Rev. B **83**, 121411 — Published 28 March 2011

DOI: [10.1103/PhysRevB.83.121411](https://doi.org/10.1103/PhysRevB.83.121411)

Strictly One-Dimensional Electron System in Au Chains on Ge(001) Revealed By Photoelectron K-Space Mapping

S. Meyer¹, J. Schäfer¹, C. Blumenstein¹, P. Höpfner¹, A. Bostwick²,
J.L. McChesney², E. Rotenberg² and R. Claessen¹

¹*Physikalisches Institut, Universität Würzburg, 97074 Würzburg, Germany*

²*Advanced Light Source, Lawrence Berkeley National Laboratory, Berkeley 94720, California, USA*

ABSTRACT

Atomic nanowires formed by Au on Ge(001) are scrutinized for the band topology of the conduction electron system by k-resolved photoemission. Two metallic electron pockets are observed. Their Fermi surface sheets form straight lines without undulations perpendicular to the chains within experimental uncertainty. The electrons hence emerge as strictly confined to one dimension. Moreover, the system is stable against a Peierls distortion down to 10 K, lending itself for studies of the spectral function.

PACS numbers: 73.20.At, 68.37.Ef, 71.10.Pm, 73.20.Mf

Self-organized atomic chains on semiconductors offer a variety of architectures, and provide model systems to study exotic physics in a nearly one-dimensional (1D) situation. Representatives include In chains on Si(111) [1], Au on Si(557) and (553) [2,3], and the recent addition of Au chains on Ge(001) [4]. Such chains with tunable properties are in focus as critical test of predictions from solid state theory. This pertains, e.g., to the Peierls instability, where a charge density wave (CDW) leads to a metal-insulator transition [5]. Alternatively, for strictly 1D systems, a correlated electron state known as Luttinger liquid is proposed [6], not found in surface systems thus far.

The key technique to address these issues is angle-resolved photoemission (ARPES). As paramount criterion for a CDW, a nesting condition must exist in a Fermi surface of quasi-1D character, accompanied by energy gaps. CDW formation was reported, e.g., for In/Si(111) [1] at moderate cooling to ~ 200 K [1,7]. Since fluctuations hinder an ideal 1D system from ordering [5], significant inter-chain coupling is required to stabilize the Peierls phase. In ARPES, a half-filled band with quasi-1D character is identified [1]. The higher-dimensional coupling is enhanced by two additional metallic bands with noticeable lateral dispersion, which are also affected by the gap opening [8]. Hence, a realistic situation with multiple bands drastically modifies a naive Peierls picture, while inhibiting formation of an exotic 1D electron liquid.

A claim of non-Fermi liquid physics was made for Au/Si(557) nanowires [2], based on an alleged spin-charge separation, yet subsequent ARPES work excluded this by revealing two conventional electron bands [9]. Moreover, small energy gaps are observed [10], pointing at a Peierls-type instability. Thus, the search for atomic chains with a highly 1D confined electron system devoid of CDW instabilities is still ongoing. In this respect, the noble metal chains on Ge(001) attract attention [4,11,12]. The recently discovered Au chains [4] have a uniquely elevated architecture and a pronounced spatial separation, suggestive of low inter-chain coupling. This spurs heightened interest in the resulting degree of electronic 1D character. STM investigations can provide at best a qualitative indication [13]. Yet, except for ambiguous low-statistics data [14], high-resolution ARPES Fermi surface mapping to address the dimensionality, manifold bands, nesting conditions, and potential energy gaps versus unusual line shapes is missing to date.

In this report, we present ARPES k-space mapping of these chains at 15 K, which reveals a novel band topology that significantly differs from all previous nanowire systems. It represents the first *single band* system, with two electron pockets on either side of the Brillouin zone. The Fermi surface consists of *parallel lines*, with possible variations from 1D behavior below detection limit. The incommensurate

band filling does not support a simple Peierls scenario, and a CDW is absent in electron diffraction down to 10 K.

Experimentally, Au was deposited onto n-doped Ge(001) at a substrate temperature of ~ 500 °C, which induces self-organized nanowire growth [4]. ARPES at 15 K was performed at the Advanced Light Source at beamline 7.0.1. The total energy resolution with a Scienta R4000 analyzer was set to ~ 30 meV at a photon energy of $h\nu = 100$ eV.

A salient feature of the nanowires, seen in STM Fig. 1(a), is that they are raised above the substrate [15]. The lateral spacing amounts to 1.6 nm. Two orientation domains (rotated by 90°) result from terrace steps of the substrate. The Au/Ge(001) chains lend themselves to ARPES studies because they exhibit excellent long-range order, reflected in their $c(8\times 2)$ low-energy electron diffraction (LEED) pattern [4].

An overview of the Fermi surface is presented in Fig. 1(b). Note that the square structure solely results from the dual domains; nonetheless the respective sheets are well separated from their rotated counterparts. The $c(8\times 2)$ surface Brillouin zone (SBZ) in Fig. 1(b) is a stretched hexagon of $\pm 0.42 \text{ \AA}^{-1}$ extent on the 1D axis to the zone boundary (ZB). Photoemission intensities are remarkably suppressed in higher SBZs, which we ascribe to optical transition matrix element effects which can cause significant modulations [16]. Already in this coarse-grid overview one observes a strikingly linear shape of the Fermi surface sheets, to be studied in detail below. This clearly disproves an earlier interpretation as a two-dimensional metallic state [14].

The central cut through $\bar{\Gamma}$ in Fig. 2(a) shows the band situation along the chains. By variation of photon energy the surface character of the bands is identified, and at $h\nu = 100$ eV the Ge bulk bands are tuned away. Two shallow electron pockets are located on either side of $\bar{\Gamma}$. Faint intensity is observed below them at higher binding energies, relating to deeper lying bands. The band situation near the Fermi surface of a single nanowire domain is sketched in Fig. 2(b), consisting of two troughs formed by the electron pockets.

These bands are of roughly symmetric shape with a band minimum at $\sim 0.20 \text{ \AA}^{-1}$, located approximately at half the distance to the ZB. No such surface states are known from bare Ge(001) [17], so they must originate from the chain reconstruction. The Fermi level crossings on either side of $\bar{\Gamma}$ are spaced by $\sim 0.12 \text{ \AA}^{-1}$. The occupied band width is ~ 100 meV, which is small compared to the ~ 500 meV range for In/Si(111) [8] and the eV-range for Au on stepped silicon [18].

In passing on the 1D axis into the 2nd SBZ, the ARPES scan coincides with the SBZ boundary line through \bar{M} , as illustrated in Fig. 2(c). The ARPES data in Fig. 2(d) reveal a parabolic hole band at \bar{M}

with weak intensity. A two-dimensional (2D) character is determined from a constant energy surface, Fig. 2(e), hence it must obey conventional Fermi liquid statistics. This 2D band forms a small hole pocket and exhibits a metallic Fermi edge (see spectra in Fig. 4(d) below). This *intrinsic* reference is used to precisely determine the *chemical potential* μ (usually termed Fermi level E_F). This is superior to a metal foil reference due to possible surface photo voltage of the sample.

It is important to note that the 2D hole band is *not* located directly at the surface. This follows from the tunneling spectroscopy data in [4], where a 2D DOS (which is constant upon energy) would lead to a step in the spectrum just above the Fermi level, yet which is not observed. Thus, the band must be localized in subsurface layers. Such substrate-derived states with hole-like dispersion are well known to occur as interface states in metal-adsorbed Ge (in addition to the adatom surface states), and are located within ~ 10 – 20 layers below the topmost layer [19,20].

Precise evaluation of the dimensionality is based on k-space mapping of the constant energy contours near μ , which host the 1D electron liquid. High-statistics Fermi surface data for samples with a domain imbalance (relating to a small incidental crystal miscut), as in Fig. 3(a), can be used to trace the dispersion. On either side of $\bar{\Gamma}$ two ridges corresponding to the Fermi vectors of the electron pocket are identified. The resulting Fermi surface lines appear very straight throughout, notably extending up to the zone boundary. The band filling f is obtained from its relation to the SBZ area as fraction of occupied k_x -range, $f \sim 0.12 \text{ \AA}^{-1} / 0.80 \text{ \AA}^{-1} \sim 0.15$ for each pocket, yielding a total band filling of ~ 0.30 .

Quantitative dispersion evaluation must rely on the momentum distribution curves (MDCs). The MDC peaks in the close-up of the Fermi surface, Fig. 3(b), are fitted with Lorentzians to determine the k_F 's. The MDC maxima are well separated, as in the example in Fig. 3(c). This analysis of the dispersion perpendicular to the chains confirms that it is virtually perfectly straight. Remaining small scatter in the k_F -positions reflects the statistical uncertainty of the MDC analysis of the two closely adjacent peaks. For each k_F contour line the accuracy of the analysis amounts to $\delta k = 0.004 \text{ \AA}^{-1}$, determined as standard deviation of 110 independent MDC fits of several data sets. This value provides a tight upper boundary for possible undulations within the Fermi surface.

In contrast, significantly larger Fermi surface curvatures are reported for, e.g., Au on Si(553) (undulation $\delta k \sim 0.03 \text{ \AA}^{-1}$) which indicates a substantial coupling between neighboring wires [3,18]. Notably, both Au-Si(553) and Au-Si(557) exhibit a complex multiband situation, and all these stepped systems exhibit lattice instabilities upon cooling. In chains on Si(111), likewise with a phase transition, also show multiple bands at the Fermi surface and a noticeable undulation for the most 1D-like band, attributed to interband interaction [8].

The shape of the Fermi contour is suggestive of various *nesting conditions* for a CDW, with distortion vectors $q_1 = 0.12 \text{ \AA}^{-1} \sim 0.15 \text{ G}$, $q_2 = 0.28 \text{ \AA}^{-1} \sim 0.35 \text{ G}$, and $q_3 = 0.52 \text{ \AA}^{-1} \sim 0.65 \text{ G}$ (where $G = 0.80 \text{ \AA}^{-1}$ is the reciprocal translation vector in 1D direction). None of them appears to be commensurate with the lattice.

The occurrence of a CDW superstructure can be probed with temperature-dependent LEED. The pattern in Fig. 4(a) at 300 K reflects the $c(8 \times 2)$ long-range order. However, at much lower temperatures no additional superstructure is observed, as evident from LEED at 10 K in Fig. 4(b). Hence formation of a CDW that would imply energy gaps can be excluded. This opens the pathway to study the non-perturbed low-energy spectral function of the 1D electron band at low temperature.

In the energy distribution curves (EDCs) of the 1D band at 15 K in Fig. 4(c), no gap opening or band backfolding occurs, although the spectral intensity is rather low near μ . This can be compared to the Fermi edge of the Ta clip in Fig. 4(d). It reflects the experimental resolution ($\sim 30 \text{ meV}$) and the small thermal broadening ($4kT \sim 5 \text{ meV}$). The metallic 2D band at \bar{M} (used as intrinsic reference for μ) closely replicates the Ta Fermi edge, albeit with slightly sloping background. In contrast, the angle-integrated spectrum in Fig. 4(d) covering the whole range of the 1D electron pocket indicates that the spectral weight is unusually suppressed in a range of $\sim 50 \text{ meV}$ below μ .

Since our investigations exclude a static Peierls distortion, one needs to consider non-Fermi liquid behavior, where the spectral weight is predicted to vanish towards μ [6]. Experimentally this was found, e.g., in the lithium purple bronze [21]. We refrain from further analysis here due to resolution limitations. Hence, it will be insightful to scrutinize the lineshape in dedicated high-resolution studies, including the temperature dependence.

In conclusion, the electron system of the Au/Ge(001) chains mapped by ARPES exhibits straight Fermi surface lines, whose 1D character is exceptionally high. At the same time, a CDW can be excluded even at 10 K. The 1D electron topology thus appears to satisfy the requirements for exotic physics. The two electron pockets call for corresponding theoretical modeling and future lineshape studies.

The authors are grateful to Y. S. Kim, L. Patthey and T. Umbach for technical support, and funding by the DFG (Scha 1510/2-1, FOR 1162) and DOE (DE-AC03-76SF00098).

Figures and Captions

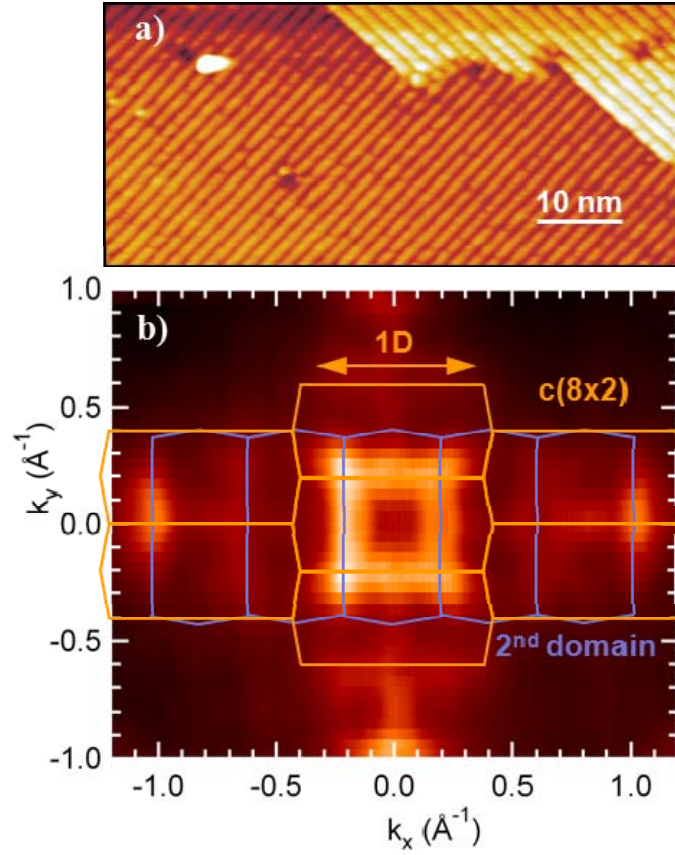


FIG. 1 (color online). a) STM image of the Au-induced nanowires (empty states, bias +1.0 V, 1.0 nA), showing two domains from terrace stacking. b) ARPES Fermi surface overview at $h\nu = 100$ eV, $T = 15$ K from dual-domain sample. The two sheets within the SBZ are rather straight perpendicular to the corresponding 1D direction. Higher SBZs appear suppressed, ascribed to matrix element effects.

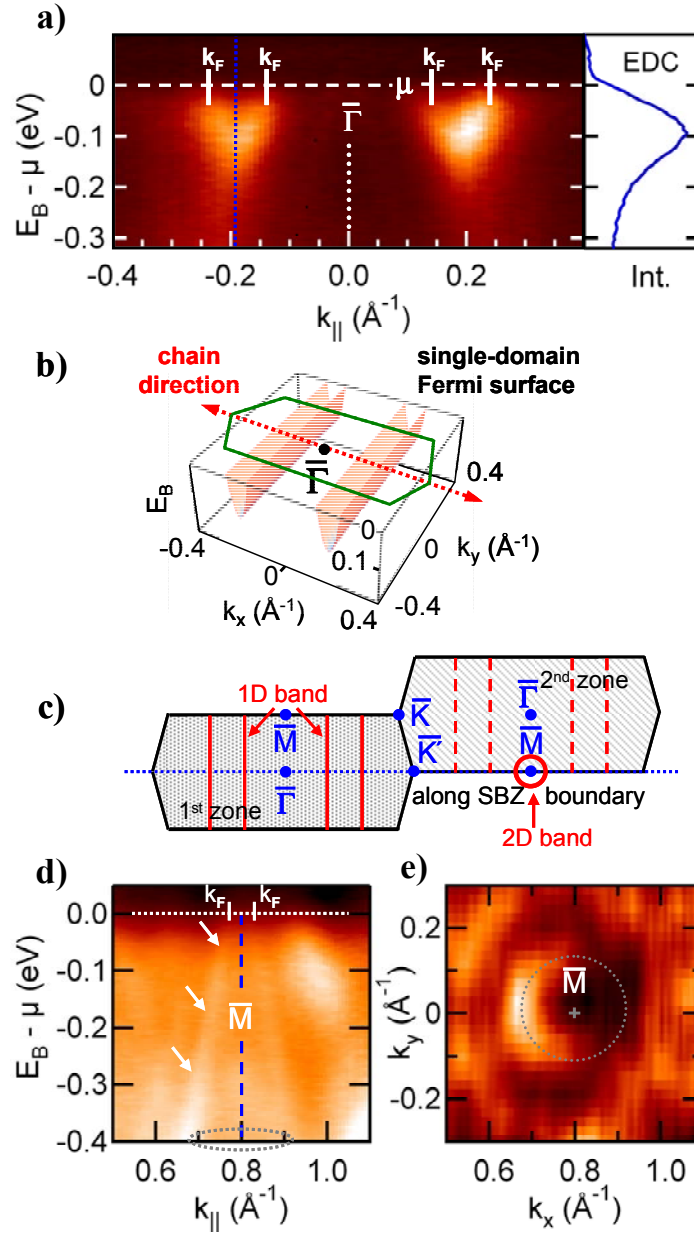


FIG. 2 (color online). a) ARPES band map at 100 eV and $T = 15$ K along chain direction through $\bar{\Gamma}$. Two shallow electron pockets are seen (energy distribution curve (EDC) taken at blue (dark grey) dotted line). b) Schematic of band situation for single-domain Au chains on Ge(001), consisting of two troughs. c) Schematic of SBZ alignment. d) Band map along $\bar{K} - \bar{M}$ of 2nd SBZ, showing a metallic hole band at \bar{M} used as intrinsic reference for μ . e) Constant energy surface at 0.4 eV binding energy, revealing the 2D character of the band at \bar{M} .

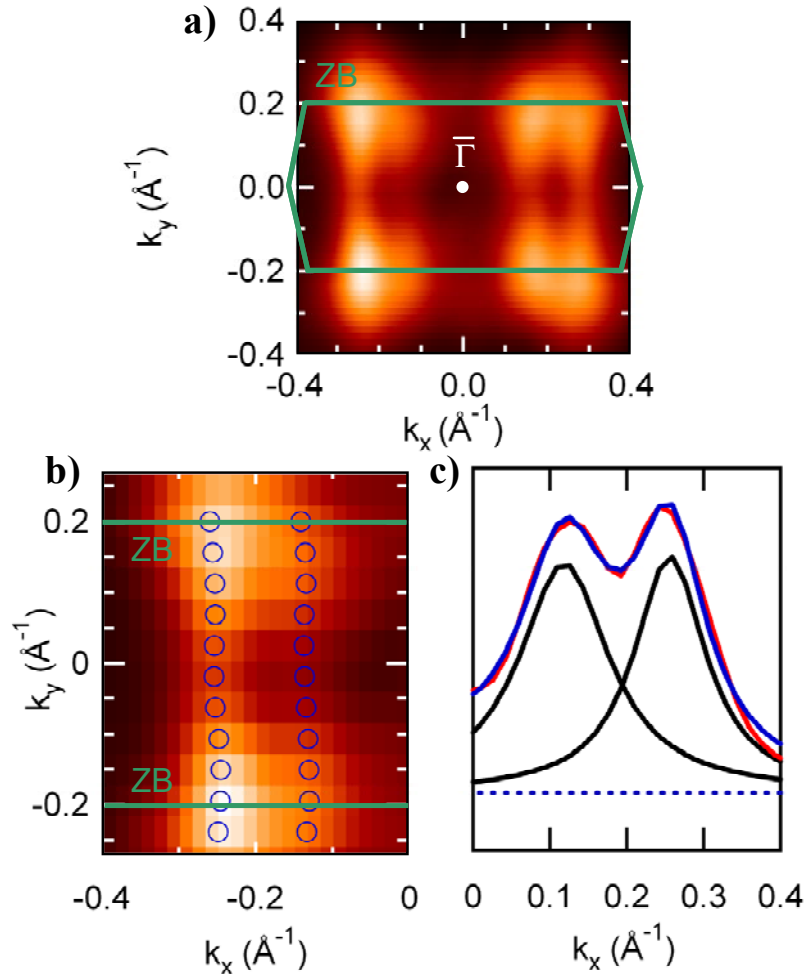


FIG. 3 (color online). a) Fermi surface (energy window μ to $\mu - 30$ meV, to compensate for low spectral weight at μ) of sample with domain imbalance. b) Close-up Fermi surface data (window μ to $\mu - 30$ meV) with k_F -positions from MDC-fits (blue/dark circles). Variations in the perpendicular k_F -lines are absent except for statistical uncertainty. c) MDC-fit for line through $\bar{\Gamma}$, showing two clearly separated k_F 's.

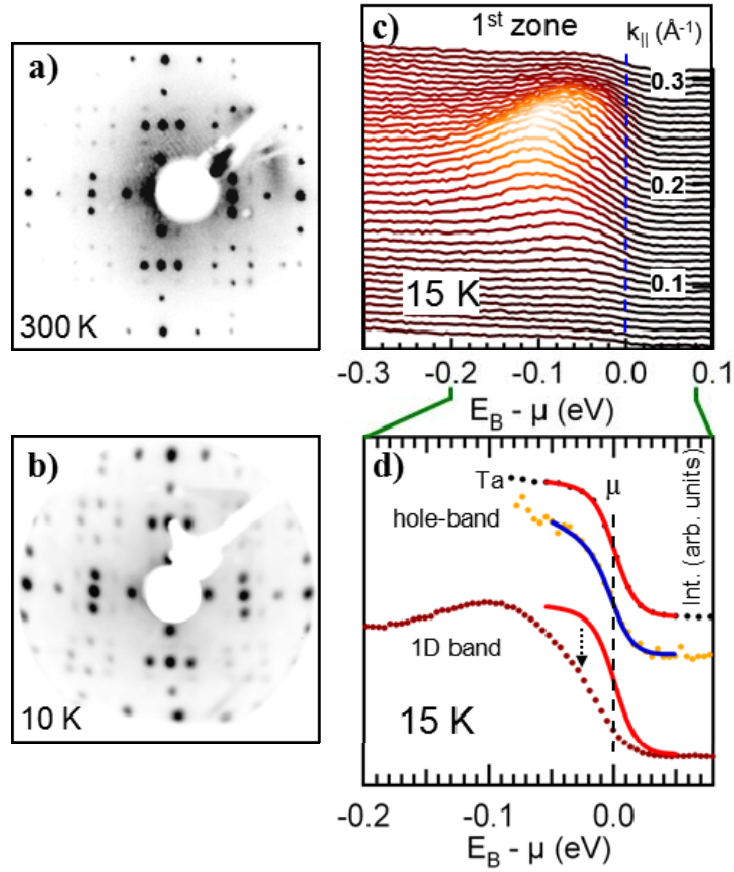


FIG. 4 (color online). a) LEED pattern (21 eV) of $c(8 \times 2)$ reconstruction (dual domain) at 300 K. b) LEED pattern (24 eV) at 10 K. It shows no additional spots so that a CDW is excluded. c) EDCs of the 1D electron pocket at 15 K (1st SBZ). d) EDCs at 15 K of Ta-foil (black dots, aligned with μ) and metallic 2D band (yellow/bright dots) used for μ -determination, fitted with resolution-broadened Fermi function including a linearly sloping density of states (red and blue overlay [solid lines]). The angle-integrated EDC (0.10 - 0.30 Å⁻¹) of the 1D band (lowest dotted line) deviates from the metallic Fermi edges (red [solid] line: Ta Fermi fit overlay), exhibiting suppressed spectral weight within ~ 50 meV below μ .

REFERENCES

-
- [1] H. W. Yeom, S. Takeda, E. Rotenberg, I. Matsuda, K. Horikoshi, J. Schaefer, C. M. Lee, S. D. Kevan, T. Ohta, T. Nagao, and S. Hasegawa, Phys. Rev. Lett. **82**, 4898 (1999).
- [2] P. Segovia, D. Purdie, M. Hengsberger & Y. Baer, Nature **402**, 504 (1999).
- [3] J. N. Crain, A. Kirakosian, K. N. Altmann, C. Bromberger, S. C. Erwin, J. L. McChesney, J.-L. Lin, and F. J. Himpsel, Phys. Rev. Lett. **90**, 176805 (2003).
- [4] J. Schäfer, C. Blumenstein, S. Meyer, M. Wisniewski, and R. Claessen, Phys. Rev. Lett. **101**, 236802 (2008).
- [5] G. Grüner, *Density Waves in Solids*, Addison-Wesley Publishing, Reading (1994).
- [6] J. Voit, Rep. Prog. Phys. **58**, 977 (1995).
- [7] J. R. Ahn, P. G. Kang, K. D. Ryang, and H. W. Yeom, Phys. Rev. Lett. **95**, 196402 (2005).
- [8] J. R. Ahn, J. H. Byun, H. Koh, E. Rotenberg, S. D. Kevan, and H. W. Yeom, Phys. Rev. Lett. **93**, 106401 (2004).
- [9] R. Losio, K. N. Altmann, A. Kirakosian, J.-L. Lin, D. Y. Petrovykh, and F. J. Himpsel, Phys. Rev. Lett. **86**, 4632 (2001).
- [10] J. R. Ahn, H. W. Yeom, H. S. Yoon, and I. - W. Lyo, Phys. Rev. Lett. **91**, 196403 (2003).
- [11] J. Schäfer, D. Schrupp, M. Preisinger, and R. Claessen, Phys. Rev. B **74**, 041404 (R) (2006).
- [12] A.A. Stekolnikov, F. Bechstedt, M. Wisniewski, J. Schäfer, and R. Claessen, Phys. Rev. Lett. **100**, 196101 (2008).
- [13] A. Van Houselt *et al.*, Phys. Rev. Lett. **103**, 209701 (2009); J. Schäfer *et al.*, Phys. Rev. Lett **103**, 209702 (2009).
- [14] K. Nakatsuji, R. Niikura, Y. Shibata, M. Yamada, T. Iimori, and F. Komori, Phys. Rev. B **80**, 081406(R) (2009).
- [15] J. Schäfer, S. Meyer, C. Blumenstein, K. Roensch, R. Claessen, S. Mietke, M. Klinke, T. Podlich, R. Matzdorf, A. A. Stekolnikov, S. Sauer and F. Bechstedt, New J. of Physics **11**, 125011 (2009).
- [16] S. Hüfner, *Very High-Resolution Photoelectron Spectroscopy*, Chapter 6, Springer-Verlag, Berlin (1998).
- [17] K. Nakatsuji, Y. Takagi, F. Komori, H. Kusunohara and A. Ishii Phys. Rev. B **72**, 241308(R) (2005).
- [18] J. N. Crain, J. L. McChesney, F. Zheng, M. C. Gallagher, P. C. Snijders, M. Bissen, C. Gundelach, S. C. Erwin, and F. J. Himpsel, Phys. Rev. B **69**, 125401 (2004).

-
- [19] S.-J. Tang, T.-R. Chang, C.-C. Huang, C.-Y. Lee, C.-M. Cheng, K.-D. Tsuei, H.-T. Jeng, and C.-Y. Mou, Phys. Rev. B **81**, 245406 (2010).
- [20] Y. Ohtsubo, S. Hatta, K. Yaji, H. Okuyama, K. Miyamoto, T. Okuda, A. Kimura, H. Namatame, M. Taniguchi, and T. Aruga, Phys. Rev. B **82**, 201307 (R) (2010).
- [21] F. Wang, J. V. Alvarez, S.-K. Mo, J. W. Allen, G.-H. Gweon, J. He, R. Jin, D. Mandrus, and H. Höchst, Phys. Rev. Lett. **96**, 196403 (2006).